

ORIGINAL ARTICLE

Open Access

Structural studies of NiTe₂ thin films with the influence of amino additives

T Joseph Sahaya Anand*, Mohd Zaidan, Mohd Asyadi Azam and Zolkepli Buang

Abstract

Background: Nickel, one of the transition metals synthesised with chalcogenides such as Se, S and Te with possible combinations of nickel chalcogenides such as NiS₂, NiSe, NiSe₂ and Ni₃Se₂. The combination of nickel and telluride are the fewest being observed due to the nature of tellurium that is relatively heavier than both sulphur and selenium, thus poorly-adhesive onto the substrate.

Methods: Therefore, NiTe₂ thin film is being synthesised onto the indium tin oxide (ITO) coated glass substrates with the complex additives (Triethanolamine, TEA and ethylenediaminetetraacetic acid, EDTA) and their properties are studied. The present work is focusing on the NiTe₂ synthesise through electrochemical route.

Results: Cyclic voltammetry experiments have been done prior to electrodeposition in order to get the electrodeposition potential range. The observable reduction range is between -0.9-(-1.1) V with 5-10 min induction period of full thin film distribution depending upon the electrolyte conditions.

Conclusion: The electrodeposition is carried out using the potentials in the reduction region, producing the well-adherent, well-distributed and dark-coloured thin films. Structural studies confirm the presence of NiTe₂ in electrolyte containing TEA with crystallite sizes lying on the 9-20 nm range.

Keywords: Thin film; Electrodeposition; Additives; Nickel telluride; Structural studies

Background

There are many synthesis routes of thin-film solar cells namely spray pyrolysis, pulsed laser deposition (PLD), chemical bath deposition, magnetron sputtering, molecular beam epitaxy and thermal evaporation which require the use of expensive machines, thus involving the high capital cost (Ilican et al. 2008; Patel 2012). Electrodeposition is introduced to cater the fabrication of thin films cost-effectively. Ability of large-scale deposition in complex shape, minimum waste of component and easy monitoring are among the advantages offered by this method (Shariza & Anand 2011; Anand 2009). Depending upon the type of additive, the film properties such as optical absorption, thermal stability, structure, morphology and adhesion onto the substrate has been studied (Junlabhut et al. 2013; Tayal et al. 2013; Vajargah et al. 2013; Anand & Shariza 2012). Solar cell is one of the promising alternative green energy sources that can

provide free electricity when sunlight is converted. The absorbent materials and their synthesis methods are subject of interest mainly due to solar panel installation cost despite of free electricity generated. The well-known silicon solar cells made, either amorphous or polycrystalline, are good in conversion efficiency up to 17%, but their high cost drives the researchers to look for new materials (Xin et al. 2012). Semiconducting materials in thin film form such as InP, SnO₂ and ZnO are being studied as the alternative materials, but are not commercialised due to their poor conversion efficiency. Another group of semiconductor compounds known as transition metal chalcogenides (TMC) have been developed to be used as the absorbent materials. Consisting of transition metals and chalcogenides (S, Se and Te), they show promising solar absorbent properties such as semiconducting band gap, good adhesion to substrate and good conversion with better cost-effectiveness. There are many TMC compounds synthesised, including copper indium selenide (CIS), CdS, CdTe, etc. (Balakrishnan & Muthusamy 2011; Radu et al. 2011).

* Correspondence: anand@utem.edu.my

Department of Engineering Materials, Faculty of Manufacturing Engineering, Universiti Teknikal Malaysia Melaka (UTeM), Durian Tunggal, Melaka 76100, MALAYSIA

Table 1 The electrolytes prepared based on three different conditions

Electrolyte	Without additive	With EDTA	With TEA
Molarity (M)	0.015 NiSO ₄ ·6H ₂ O + 0.003 TeO ₂	0.015 NiSO ₄ ·6H ₂ O + 0.003 TeO ₂ + 0.053	0.015 NiSO ₄ ·6H ₂ O + 0.003 TeO ₂ +
Composition of additive	-	0.053 M EDTA	1.0 M TEA
Acidic/basic condition	Base (pH 10)	Acidic (pH 3)	Base (pH 10)

Sources: Aricò et al. 1997; Saloniemi et al. 1998; Takahashi et al. 1994.

Thin films referred as transition metal chalcogenides (TMC) have alternatively been used as the absorbent material for solar cells to replace the widely used silicon. Though many thin films of oxides, sulphides and selenide have been synthesised, only few studies of telluride thin films such as Bi₂Te₃, Hg_{1-x}Cd_xTe, CdTe, CoTe and Ag₂Te have been reported (Asokan et al. 2008; Peng et al. 2003; Sander et al. 2002). As one of the transition metal chalcogenides, nickel telluride, NiTe₂, has been deposited in the form of thin film onto indium tin oxide (ITO)-coated glass substrates to be further developed into thin film solar cell. Though there is no reported literature about the use of NiTe₂ to function as a solar cell, this has the high potential to be the candidate material of a solar cell. The syntheses of telluride thin films involve several techniques such as physical vapour deposition (PVD), metal organic vapour chemical deposition (MOCVD), solvothermal methods, coreduction method (in-situ) and electrodeposition (Peng et al. 2003). The PVD technique is excellent for good-quality film growth but is difficult to scale up (Anand et al. 2013a). The absorber layers for high-quality devices are typically synthesised via high vacuum deposition processes such as co-evaporation that is costly due to initial cost of equipment and production of vacuum (Ikeda et al. 2011).

Therefore, there is a great interest in developing non-vacuum, large-scale and low-cost technique such as electrodeposition (Anand et al. 2013a) for preparing NiTe₂ thin films. Low-temperature processing results in the cost-effectiveness of this technique. Also, there is negligible waste of chemicals with better utilisation efficiencies. Semiconducting tellurides have great potential applications in optoelectronic devices including photovoltaic devices, light emitting diodes (LED), biological sensors and nanoscale electronics (Sander et al. 2002; Ling et al. 2010). NiTe₂ in the form of nanorods were successfully synthesised through solvothermal method at temperatures (160°C and 180°C for 10 and 15 h, respectively) (Bin et al. 1999). Besides, NiTe₂ nanoflakes and their self-assembled nanoflake arrays (1-D

nanostructures) were prepared by a single-step hydrothermal method (Ling et al. 2010). The single-step electrodeposition is the most desirable way to simplify thin film fabrication, thus would be used to synthesise NiTe₂ thin films (Anand et al. 2013a). The use of additives in thin film syntheses has been implemented where hexagonal NiTe₂

Table 2 The tabulation of additive concentration

Additive	Concentration (M)				
	1	2	3	4	5
EDTA	0	0.013	0.026	0.052	0.104
TEA	0	0.050	0.100	0.150	0.200

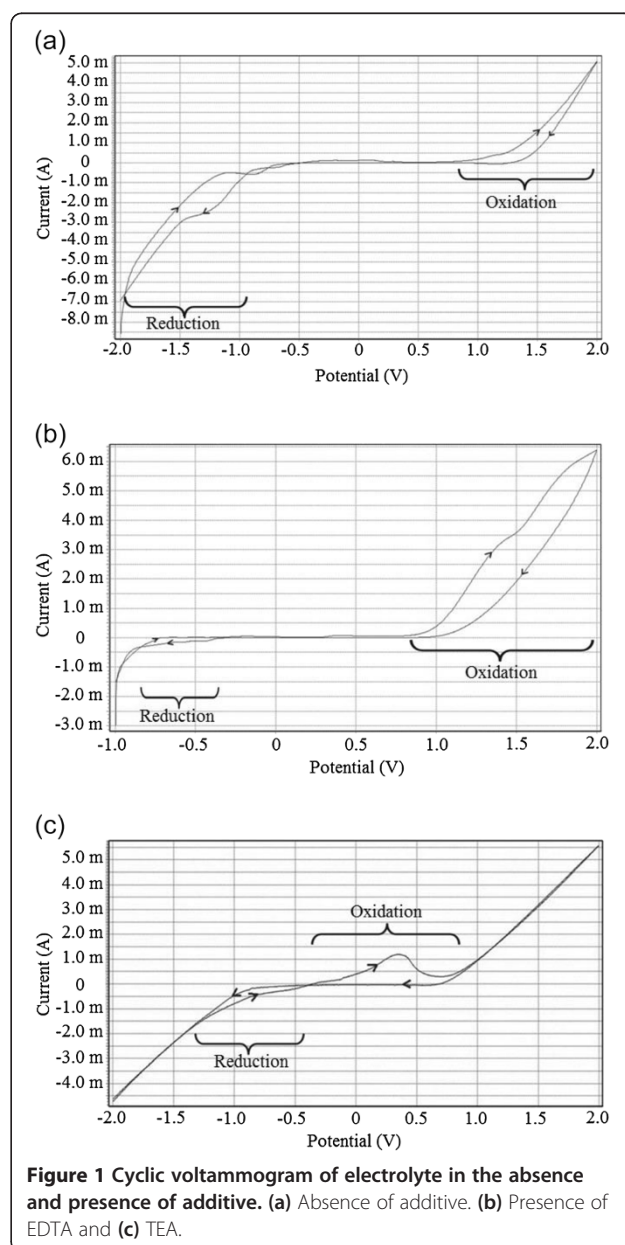


Figure 1 Cyclic voltammogram of electrolyte in the absence and presence of additive. (a) Absence of additive. (b) Presence of EDTA and (c) TEA.

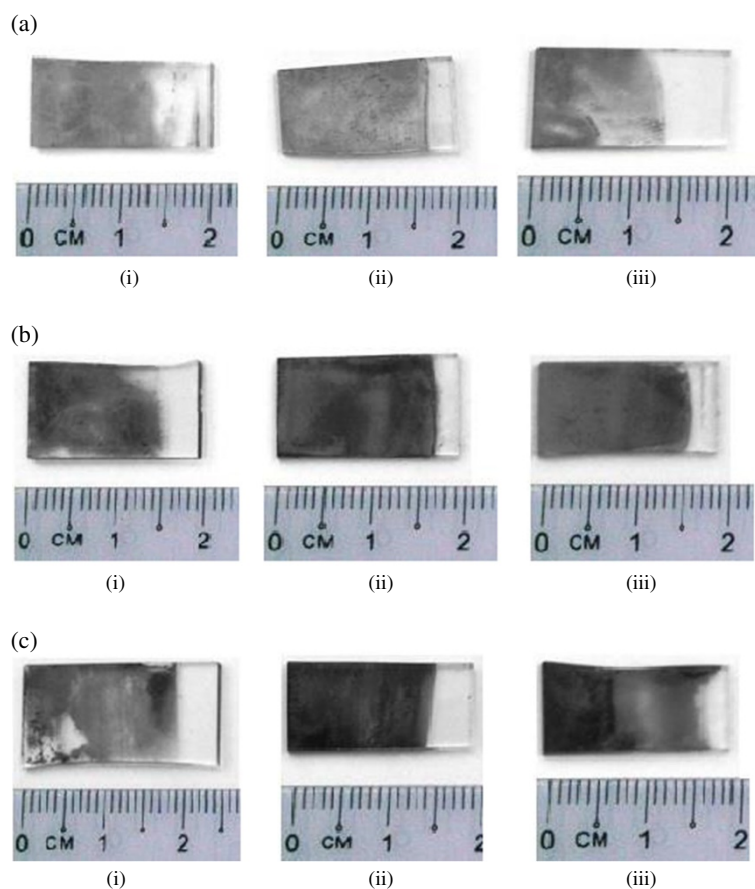


Figure 2 Appearance of thin films at 30-min deposition time. With (a) no additive at (i) -0.9 , (ii) -1.0 and (iii) -1.1 V deposition potential; (b) EDTA at (i) -0.9 , (ii) -1.0 and (iii) -1.1 V deposition potential and (c) TEA at (i) -0.9 , (ii) -1.0 and (iii) -1.1 V deposition potential.

nanoplates have been synthesised through an ethylenediaminetetracetic acid (EDTA)-assisted hydrothermal reaction and NiSe_2 thin films have been obtained via triethanolamine (TEA)-assisted electrodeposition techniques (Liu et al. 2009; Anand et al. 2013b). In this paper, the preparation of NiTe_2 thin films by the electrodeposition technique has been presented in different electrolyte conditions, deposition potential and deposition time with the use of both TEA and EDTA additives, separately. The effect of these additives has been thoroughly investigated prior to thin film characterisations.

Methods

Thin-film fabrication began with the preparation of the substrates. The conductive ITO-coated conducting glass substrates with $7 \Omega/\text{cm}^2$ resistivity were ultrasonically cleaned in ethanol and subsequently in distilled water for 10 min each at 60°C (Anuar et al. 2010; Hesson 2012). Then, they are dried at 60°C (Zhuang et al. 2006). The experiment then continues with the preparation of electrolytes as specified in Table 1. The standard three-electrode cell configuration was used

where ITO-coated glasses were used as the substrates (working electrode) of NiTe_2 thin films (Ikeda et al. 2011). The graphite and Ag/AgCl (3.33 M KCl) electrodes were used as counter and reference electrode, respectively (Takahashi et al. 1994). Both cyclic voltammetry (CV) and electrodeposition were run by using DC Voltammetry System (Princeton Applied Research - VersaSTAT 3) driven by VersaStudio software.

The cyclic voltammetry was run in the standard -2 to 2 V potential range with 30 min and 0.02 V/s being the time and scan rate, in order to get the most appropriate potential range of electrodeposition with respect to

Table 3 The optimum additive concentration, deposition potential and deposition time

Electrolyte	Deposition potential (V)	Deposition time (min)
$0.015 \text{ M NiSO}_4 \cdot 6\text{H}_2\text{O} + 0.003 \text{ M TeO}_2$	-1.0	20 to 30
$0.015 \text{ M NiSO}_4 \cdot 6\text{H}_2\text{O} + 0.003 \text{ M TeO}_2 + 0.026 \text{ M EDTA}$	-1.1	5 to 30
$0.015 \text{ M NiSO}_4 \cdot 6\text{H}_2\text{O} + 0.003 \text{ M TeO}_2 + 0.1 \text{ M TEA}$	-1.0	10 to 30

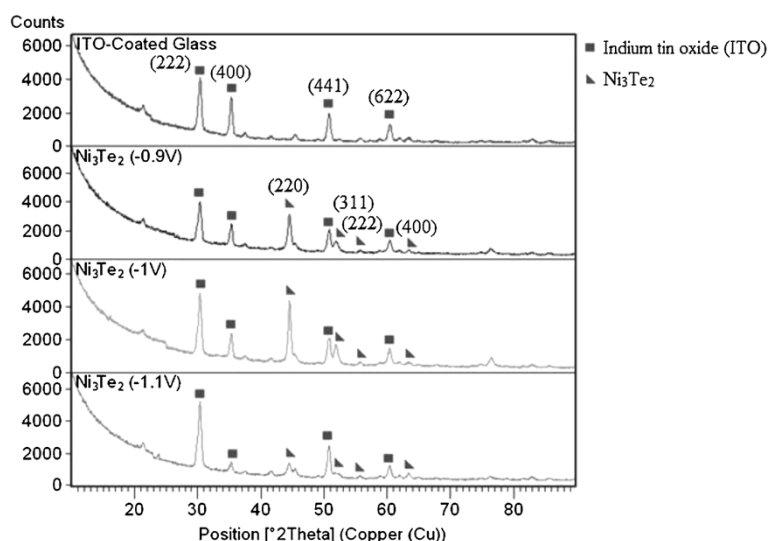


Figure 3 X-ray diffractograms of thin film for different potentials (no additive, 30 min).

electrolyte conditions. The temperature was controlled to $40^{\circ}\text{C} \pm 2^{\circ}\text{C}$ (Anand et al. 2013b). The first lower peak and subsequent upper peak of cyclic voltammograms represent the reduction and oxidation processes of the ions in electrolyte respectively. Once the potential range was obtained, the electrodeposition experiments had been conducted in three different electrolyte conditions as described in Table 1 in order to determine the optimum deposition potential and deposition time of NiTe_2 thin-film electrodeposition.

The effect of additive concentration had been studied by varying the concentration of both EDTA and TEA with optimum deposition potential and time as described in Table 2. To observe the crystal structure of the thin film,

X-ray diffraction (XRD) analysis has been done by using PANalytical XPERT PROMPD PW 3040/60 diffractometer (Almelo, The Netherlands) using monochromatic $\text{Cu K}\alpha$ radiation ($\lambda = 1.5418 \text{ \AA}$) at 2θ angles in the range of 0° to 90° (Anand et al. 2013b).

Results and discussion

Cyclic voltammetry and optimum parameters of thin-film electrodeposition

As shown in Figure 1 (a,b,c, both reduction and oxidation process take place during CV. In the absence of additive, the cathodic current onset is observable at about -1.9 V during the forward scan, followed by a steady current rise up to about -1.1 V . The deposition reaction was re-verified

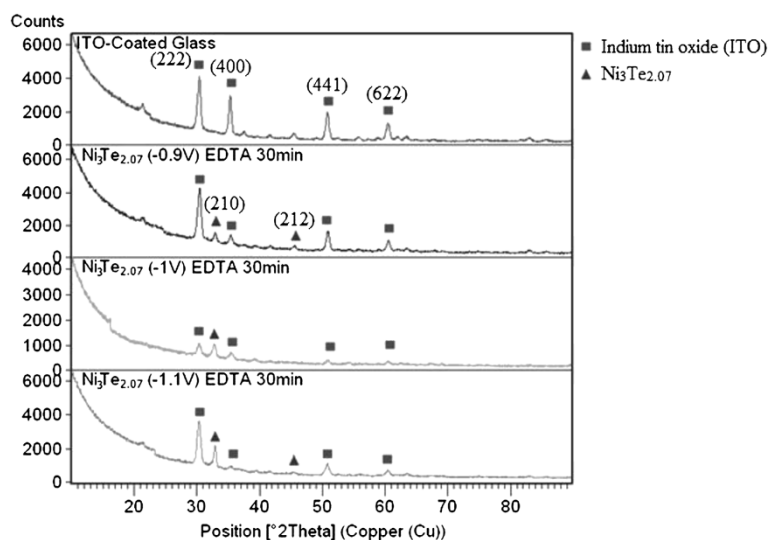
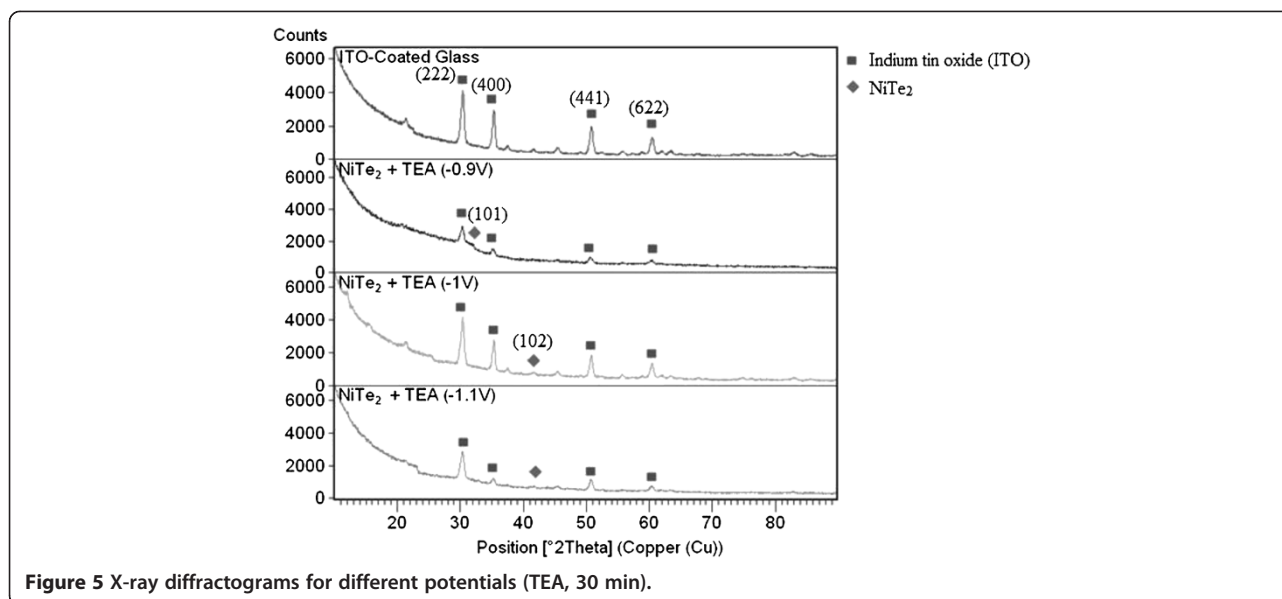


Figure 4 X-ray diffractograms of thin film for different potentials (EDTA, 30 min).



by the reverse scan where the interception currents occurred at -0.5 , -0.75 and -0.9 V. During the reverse scan, co-deposition occurs in the negative potential range with the decreasing current value as the deposition potential is scanned towards more negative value (cathodic region) (Zainal et al. 2005). On the other hand, by reversing the potential scanning, the reduction process takes place in a relatively short range in the presence of EDTA, between -0.3 and -0.8 V. These potentials are not appropriate for electrodeposition, causing the overload of the three-cell electrode system, showing that acidic electrolyte (in the presence of EDTA) is not suitable in synthesising the NiTe_2 thin films.

As shown in Figure 1c, the forward scan raises and intercepts at -1.25 V suggesting a reduction process. The reduction of nickel (II) ions to form a solid nickel compound onto the substrate occurs in this reduction region (Zainal et al. 2005). Thus, the electrodeposition potential lies within this region, between -0.4 and -1.25 V. It appears that the -1.1 to -1.0 V was the most suitable potential once a few electrodeposition experiments had been conducted. The current value is increased as the deposition potential is scanned towards more positive value (anodic region). During the reverse scan, co-deposition

occurs in the negative potential range. The deposition of both nickel (Ni) and tellurium (Te) on the conductive glass surface continued until all the equilibrium potential is achieved at another interception between forward and reverse scan at about -1.25 V versus Ag/AgCl. The current rise at about -0.4 V, followed by a large anodic wave indicates the oxidation of the nickel compound (Zainal et al. 2005). A few overloads have occurred due to the use of inappropriate potential during electrodeposition, preventing the completion of film deposition. The films deposited in the absence of an additive have poor film adhesion and distribution in grey where the film distribution is not uniform at all potentials shown in Figure 2a. TEA results in black-coloured uniform film formation, whereas the dull-grey-coloured uniform films are observable in the case of the use of the EDTA additive as shown in Figure 2b,c, respectively. It was found that EDTA works well in producing uniform and bright coatings (Haiyan et al. 2011). Based on the film adhesion, uniformity and distribution, the optimum deposition potential and time are concluded in Table 3.

Table 4 The comparison of ITO experimental 'd' values with its JCPDS data

Angle, 2θ ($^\circ$)	Standard (\AA)		Experimental 'd'
	(h k l)	'd' _{JCPDS}	
30.273	(2 2 2)	2.950	2.945
35.165	(4 0 0)	2.550	2.543
50.978	(4 4 1)	1.790	1.797
59.940	(6 2 2)	1.542	1.531

Table 5 Comparison of experimental 'd' values with JCPDS data for Ni_3Te_2 (no additive, 30 min)

Angle, 2θ ($^\circ$)	(h k l)	Standard (\AA) 'd' _{JCPDS}	Experimental (\AA)		
			-0.9 V	-1.0 V	-1.1 V
26.832	(1 1 1)	3.320	3.478	3.374	3.249
31.016	(2 0 0)	2.881	2.941	2.942	2.941
44.439	(2 2 0)	2.037	2.034	2.034	2.036
52.683	(3 1 1)	1.736	1.762	1.796	1.798
55.187	(2 2 2)	1.663	1.647	1.648	1.649
64.628	(4 0 0)	1.441	1.439	1.438	1.436

These values are compared with respect to different deposition potentials.

A few electrodeposition experiments using EDTA in different concentrations revealed that the dark-grey film distribution was in good uniformity within the concentration range with 0.0265 M being the best EDTA concentration; however, the film adhesion started to become poor at 0.053 M and above. In the case of TEA, the optimum concentration was 0.1 M. Both 0.15 and 0.20 M TEA resulted in darker and poor-adherent films. On the contrary, the brighter films were acquired using 0.05 M TEA, but their adhesions were poor as well.

Structural studies

The XRD patterns of the electrodeposited nickel telluride thin film on ITO-coated glass substrate is shown in Figures 3,4,5. Due to the amorphous nature of the ITO-coated glass substrate, the diffractograms begin with a high peak intensity. The XRD peaks identified in the figure have been indexed with the help of the Joint Committee of Powder Diffraction Standards (JCPDS) file and the corresponding data are summarised in Tables 4,5,6,7. The sharp diffractogram peaks reveal that the nickel telluride films deposited on ITO-coated glass substrates are polycrystalline in nature (Shariza & Anand 2011). In the absence of an additive, the peaks are identified as (220), (311), (222) and (400) planes of Ni₃Te₂ and (222), (400), (441) and (622) planes of ITO (Zainal et al. 2005; Haiyan et al. 2011). The structural features fit into the cubic structure of Ni₃Te₂ films with lattice parameter values $a = b = c = 0.5760$ nm which are in good agreement with the standard values (JCPDS, ICDD, Card No. 00-019-0845). However, the stoichiometry is not in the film prepared without the influence of additive.

It can be seen in Figure 3 that at all deposition potentials, the peaks of ITO are more prominent in intensity. At -1 V deposition time, the film peak intensities are at the highest, especially that of (220) and (311) planes at $2\theta = 44.439^\circ$ and 52.683° , showing that -1 V is the optimum potential at this particular electrolyte condition. ITO peaks at $2\theta = 50.978$ have shrunk at -0.9 and -0.1 V due to the growth of (311) plane films which has surmounted over the ITO. The interplanar distances 'd' corresponding to different $h k l$ planes have been calculated from the X-ray diffractograms while the crystallite

Table 6 Comparison of experimental 'd' values with JCPDS data for Ni₃Te_{2.07} (with EDTA, 30 min)

Angle, 2θ (°)	(h k l)	Standard (Å)	Experimental (Å)		
		'd' _{JCPDS}	-0.9 V	-1.0 V	-1.1 V
33.421	(2 1 0)	2.679	2.729	2.734	2.732
37.917	(0 1 2)	2.371	2.399	-	2.416
45.116	(2 1 2)	2.008	1.992	1.983	2.003
56.246	(2 2 1)	1.634	1.648	1.645	1.642

These values are compared with respect to different deposition potentials.

Table 7 Comparison of experimental 'd' values with JCPDS data for NiTe₂ (with TEA, 30 min)

Angle, 2θ (°)	(h k l)	Standard (Å)	Experimental (Å)		
		'd' _{JCPDS}	-0.9 V	-1.0 V	-1.1 V
31.704	(1 0 1)	2.820	2.807	-	-
43.917	(1 0 2)	2.060	1.993	1.996	2.078
79.551	(2 0 3)	1.204	1.213	1.212	1.214

These values are compared with respect to different deposition potentials.

sizes are calculated from the measurement of full-width at half-maximum (FWHM) in different X-ray peaks, giving the values in the range of 9 to 20 nm.

Figure 4 shows the XRD patterns of non-stoichiometric nickel telluride, Ni₃Te_{2.07} thin film deposited in the presence of EDTA corresponding to different deposition potentials. The peaks are identified as (210) and (212) planes of Ni₃Te_{2.07}. The structural features fit into the orthorhombic structure of the Ni₃Te_{2.07} with lattice parameters values $a = 0.7544$, $b = 0.3796$ and $c = 0.6073$ nm which are in good agreement with the standard values (JCPDS, ICDD, Card No. 00-019-0847). Also, it can be seen that the film peak is relatively fewer at -1.0 V as compared to the ones at -0.9 and -1.1 V. The film peak intensity of (210) plane is the highest at -1.1 V suggesting that -1.1 V is the optimum potential at this electrolyte condition. The ITO peaks having (400), (441) and (622) planes show the observable decrease in intensity at each potential.

The film peaks matching the stoichiometric NiTe₂ are detected in Figure 5 diffractograms. The peaks are identified as (101) and (102) planes of NiTe₂. The structural features fit into the hexagonal structure of NiTe₂ with lattice parameter values $a = b = 0.3843$ nm and $c = 0.5265$ nm which are in good agreement with the standard values (JCPDS, ICDD, Card No. 00-008-0004; Rotlevi et al. 2001). At $2\theta = 31.704$ at -0.9 V and $2\theta = 43.917$ at both -1.0 and -1.1 V, only one peak is obviously detected each with slightly higher intensity peak at -1.0 V, suggesting its optimum potential. The (400), (441) and (622) planes of ITO peaks relatively decrease at both -0.9 and -1.1 V.

Conclusion

Through the electrodeposition route, NiTe₂ thin films have been successfully deposited onto ITO-coated glass substrates at -1.1 to -1.0 deposition potential range and 5 to 30 minutes deposition time. The presence of TEA in basic condition results in black-coloured and well-distributed stoichiometric films with good adhesion, enabling the optimum solar energy absorption as proven by structural studies and film appearance observation. It is found that the acidic electrolyte is not suitable for depositing NiTe₂ thin films as proven by the inappropriate reduction range and poor adhesion of films.

Competing interests

The authors declare that they have no competing interests.

Authors' contributions

TJSA is the main author who contributed and organized the entire research and confirmed the obtained results including the critical discussion. MZ is a postgraduate student who carried out most of the experiment, MAA helped to analyse the partial data and ZB helped to check the language and critical discussion. All authors read and approved the final manuscript.

Acknowledgement

The work described in this paper was supported by Universiti Teknikal Malaysia Melaka (UTeM) and FRGS / KeTTHA sponsored research grant (Project No. FRGS/2011/FKP/TK 02/1 F00120).

Received: 14 May 2014 Accepted: 3 September 2014

Published online: 24 September 2014

References

- Anand, TJS. (2009). Synthesis and characterization of MoS₂ film for photoelectrochemical cells. *Sains Malaysiana*, 38, 85–89.
- Anand, TJS, & Shariza, S. (2012). A study on molybdenum sulphoselenide (MoS_xSe_{2-x}, 0 ≤ x ≤ 2) thin films: growth solution and its properties. *Electrochimica Acta*, 81, 64–73.
- Anand, TJS, Shariza, S, Rosli, ZM, & Thiru, S. (2013a). Optical and Mott-Schottky studies of ternary MoSSe thin films synthesized by electrochemical route. *World Applied Science Journal*, 21, 60–67.
- Anand, TJS, Zaidan, M, & Shariza, S. (2013b). Effect of additives on optical measurements of NiSe₂ thin films. *Procedia Engineering*, 53, 555–561.
- Anuar, K, Saravanan, N, Tan, WT, Ho, SM, & Teo, D. (2010). Chemical bath deposition of nickel sulphide (Ni₄S₃) thin films. *Leonardo Journal Science*, 16, 1–12.
- Aricò, AS, Silvestro, D, Antonucci, PL, Giordano, N, & Antonucci, V. (1997). Electrodeposited thin film ZnTe semiconductors for photovoltaic applications. *Advanced Performance Materials*, 4, 115–125.
- Asokan, K, Tsai, HM, Bao, CW, & Sonia, G. (2008). Effect of swift ions in Ni-Al nanocrystalline films studied by X-ray absorption spectroscopy. *Spectrochimica Acta A*, 70, 454–457.
- Balakrishnan, K, & Muthusamy, D. (2011). Determination of optimum film thickness and composition of Cu(InAl)Se₂ thin films as an absorber for solar cell applications. *World of Journal Nanoscience and Engineering*, 1, 108–118.
- Bin, L, Yi, X, Jiaying, H, Huilan, S, & Yitai, Q. (1999). Solvothermal synthesis to NiE₂ (E=Se, Te) nanorods at low temperature. *Nanostructured Materials*, 11, 1067–1071.
- Haiyan, Y, Xingwu, G, Birbilis, N, Guohua, W, & Wenjiang. (2011). Tailoring nickel coatings via electrodeposition from a eutectic-based ionic liquid doped with nicotinic acid. *Applied Surface Science*, 257, 9094–9102.
- Hesson, JR. (2012). *Fundamentals of ultrasonic cleaning high energy sound supersonics*. United States: Hessonics.
- Ikeda, S, Kamai, R, Lee, SM, Yagi, T, Harada, T, & Matsumura, M. (2011). A superstrate solar cell based on In₂(Se, S)₃ and CuIn(S₂) thin films fabricated by electrodeposition combined with annealing. *Solar Energy Materials Solar Cells*, 95, 1446–1451.
- Ilican, S, Caglar, Y, & Caglar, M. (2008). Preparation and characterization of ZnO thin films deposited by sol-gel spin coating method. *Journal of Optoelectronics and Advanced Materials*, 10, 2578–2583.
- JCPDS, ICDD. *PANalytical X'Pert HighScore*. Card No. 00-019-0845.
- JCPDS, ICDD. *PANalytical X'Pert HighScore*. Card No. 00-019-0847.
- JCPDS, ICDD. *PANalytical X'Pert HighScore*. Card No. 00-008-0004.
- Junlabhut, P, Boonruang, S, & Pecharapa, W. (2013). Optical absorptivity enhancement of SiO₂ thin film by Ti and Ag additive. *Energy Process*, 34, 734–739.
- Ling, J, Ying, JZ, & Jing, BC. (2010). Cetyltrimethylammonium bromide assisted self-assembly of NiTe₂ nanoflakes: nanoflake arrays and their photoluminescence properties. *Journal of Solid State Chemistry*, 183, 2358–2364.
- Liu, X, Hu, R, Chai, L, Li, H, & Qian, Y. (2009). Synthesis and characterization of hexagonal NiTe₂ nanoplates. *Journal of Nanoscience and Nanotechnology*, 9, 2715–2718.
- Patel, TH. (2012). Influence of deposition time on structural and optical properties of chemically deposited SnS thin films. *Open Surface Science Journal*, 4, 6–13.
- Peng, Q, Dong, Y, & Li, Y. (2003). Synthesis of uniform CoTe and NiTe semiconductor nanocluster wires through a novel coreduction method. *Inorganic Chemistry*, 42, 2174–2175.
- Radu, M, Ghenescu, V, Stan, I, Ion, L, Besleaga, C, Nicolae, A, Mitran, TL, Tazlaoanu, C, Radu, A, Porumb, O, Ghenescu, M, Gugiu, MM, & Antohe, S. (2011). Photovoltaic properties of the CdS/CdTe heterojunction solar cells before and after proton irradiation. *Chalcogenide Letters*, 8, 477–485.
- Rotlevi, O, Dobson, KD, Rose, D, & Hodes, G. (2001). Electroless Ni and NiTe₂ ohmic contacts for CdTe/CdS PV cells. *Thin Solid Films*, 387, 155–157.
- Saloniemi, H, Kanninen, T, Ritala, M, & Leskela, M. (1998). Electrodeposition of PbTe thin films. *Thin Solid Films*, 326, 78–82.
- Sander, MS, Prieto, AL, Gronsky, R, Sands, T, & Stacy, AM. (2002). Fabrication of high-density, high aspect ratio, large-area bismuth telluride nanowire arrays by electrodeposition into porous anodic alumina templates. *Advanced Materials*, 14, 665–667.
- Shariza, S, & Anand, TJS. (2011). Effect of deposition time on the structural and optical properties of molybdenum chalcogenides thin films. *Chalcogenide Letters*, 9, 529–539.
- Takahashi, M, Katou, Y, Nagata, K, & Furuta, S. (1994). The composition and conductivity of electrodeposited Bi-Te alloy films. *Thin Solid Films*, 240, 70–72.
- Tayal, A, Gupta, M, Gupta, A, Horisberger, M, & Stahn, J. (2013). Role of additives (X = Ti, Zr) in phase formation and thermal stability of Fe-X-N thin films. *Thin Solid Films*, 536, 39–49.
- Vajargah, PH, Abdizadeh, H, Ebrahimifard, R, & Golobostanfard, MR. (2013). Sol-gel derived ZnO thin films: effect of amino-additives. *Applied Surface Science*, 285, 732–743.
- Xin, G, Xuegong, Y, Kuanxin, G, Lin, C, Dong, W, & Deren, Y. (2012). Seed-assisted cast quasi-single crystalline silicon for photovoltaic application: towards high efficiency and low cost silicon solar cells. *Solar Energy Materials Solar Cells*, 101, 95–101.
- Zainal, Z, Saravanan, N, & Mien, HL. (2005). Electrodeposition of nickel selenide thin films in the presence of triethanolamine as a complexing agent. *Journal of Materials Science: Materials in Electronics*, 16, 111–117.
- Zhuang, Z, Peng, Q, Zhuang, J, Wang, X, & Yadong, L. (2006). Controlled hydrothermal synthesis and structural characterization of nickel selenide series. *Chemistry A European Journal*, 12, 211–217.

doi:10.1186/s40712-014-0018-3

Cite this article as: Anand et al.: Structural studies of NiTe₂ thin films with the influence of amino additives. *International Journal of Mechanical and Materials Engineering* 2014 **9**:18.

Submit your manuscript to a SpringerOpen® journal and benefit from:

- Convenient online submission
- Rigorous peer review
- Immediate publication on acceptance
- Open access: articles freely available online
- High visibility within the field
- Retaining the copyright to your article

Submit your next manuscript at ► springeropen.com